VOL. 13, NO. 24, DECEMBER 2018 ISSN 1819-6608
ARPN Journal of Engineering and Applied Sciences

www.arpnjournals.com

MICROWAVE ATTENUATION AND PHASE ROTATION IN SAND AND DUST STORMS - PART I

Abdul Waheed Musa and B. S. Paul
Institute of Intelligent Systems, University of Johannesburg, South Africa
E-Mail: twhid2001@yahoo.com

ABSTRACT

Microwave signal propagation may suffer attenuation and phase rotation by suspended particles during sand and dust storms (SDS) in arid and semi-arid regions of Africa and Asia. This development has received considerable interest in recent time. Thus, attenuation and phase rotation induced by SDS were investigated and models for estimating these propagation parameters are presented in this paper. Using Rayleigh method, the models were premised on the complex forward scattering amplitude of dust particles with spherical shape. Three different conditions were tested to proof the suitability of the method used. The results show that the Rayleigh approximation method is suitable and valid in determining scattering effects of dust particles with spherical shape for frequency range and dust particle sizes considered. The microwave (MW) attenuation and phase rotation expressions are proposed as functions of visibility, complex permittivity and wavelength. It was found that attenuation and phase rotation increase with increase in severity of SDS. Also, attenuation in dry dust is only influential at frequency of lower millimetric wave range or when the visibility becomes severe.

Keywords: microwave, attenuation, phase rotation, dust storms, propagation, spherical shape.

1. INTRODUCTION

Sand or dust storm is a phenomenon that occurs in arid and semi-arid regions of Africa and Asia. It is an unpleasant weather situation characterized by dust-filled air blown by strong wind over an extensive area. Dust particles from sand and dust storms (SDS) affect communication links by reducing signal quality through attenuation along the propagation path and crosstalk in dual polarized links introduced into each channel of the receiver emanating from the transmitter channel of the orthogonal polarization.

Investigators have expressed appreciable interest in the problem associated with effects of SDS on performance of the MW links [1]. This was due to the growth of terrestrial and satellite microwave systems as well as the exploration of higher frequency spectrums [2]. There is significant evolvement of new and demanding telecommunication applications because of spectral congestion of the conventional frequency bands in the past few decades. This has resulted into increased attention being paid to higher carrier frequencies for efficiency and effectiveness in information transfer rates, and to further enhance and improve miniaturized equipment and their portability. Investigations [3] have shown that scattering of MW by SDS can be attributed to factors such as severity of the SDS in terms of visibility and density, dust particle shape and size, moisture and permittivity, and the incident wave frequency. These are very important parameters in formulating MW propagation models.

In general, methods for model formulation of scattering in dust particle populations are like that of population of hydrometeors. This is because media such as the SDS and the hydrometeors are discrete and random. Generally, the impacts of SDS and their particles on propagation links are estimated by working out solution for a forward scattering amplitude function of a single (dust) particle. This could be obtained either through numerical or analytical methods [4]. Attenuation and phase rotation of MW propagation during SDS emanated from absorption and scattering of the waves by the dust particles. Therefore, microwave attenuation and phase rotation models both for equal sized distribution and exponential size distribution for spherical dust particle are proposed in this work using the forward scattering amplitude function of Rayleigh method.

One of the research issues identified and eventually tackled in this research work is the fact that where the Rayleigh methods have been used to calculate signal attenuation [5], due consideration was not given to sizes of dust particles under consideration [6] and the method was not validated against any known full solution of Maxwell's equations. Besides, some of the final expressions [7] were given in parameters difficult to quantify. Against this premise, this work takes into cognizance the validation of Rayleigh method against Maxwell's equations, dust particle shapes and suitability for particles smaller than the wavelength. It also ensures that the model expressions are given in terms of SDS visibility to represent the extent of storm's density as against the use of concentration number of SDS dust particles which are usually difficult to quantify.

Bearing in mind the limitations in applications of other scattering methods, the choice of Rayleigh scattering approximation method is borne out of the simplicity of the method and its applications to different propagation media and particle shapes.

The report of this research work is organized such that introduction is given in section 1, Rayleigh electromagnetic wave complex scattering is presented in section 2, the proposed attenuation and phase rotation models are developed and presented in section 3. Lastly, the simulation results are presented and discussed in section 4, while conclusions are drawn in section 5.

2. RAYLEIGH MICROWAVE SCATTERING

Method of Rayleigh approximation is verified to solve complex scattering at microwave bands in this section. The Rayleigh approximation method presents a solution (analytical) of the Maxwell's equations for electromagnetic waves complex scattering by dielectric particles. The Rayleigh approximation method can be expressed as:

$$\frac{2\pi a}{\lambda} \ll 1 \quad (1)$$

where

λ = the transmitting wavelength
a = the radius of the dust particle

An explanation to the expression in (1) is that the radius of the given particle is very small compared to the wavelength. For a relatively small spherical particle that is relatively small when compared to the wavelength [8], the field inside the particle is selected to be the solution of the dielectric. Thus, it can be assumed that the particle is placed in a uniform homogeneous electric field.

Second assumption is drawn from $k|\bar{m}|a \ll 1$ [9]; where $\bar{m}$is the particle refractive index and k is a propagation constant. This means that the incident field penetrates inside the particle so fast that the static polarization is observed in a short period of time when compared to the period of wave. Lastly, another simplification and assumption ensure that the external field phase is not significantly different from the phase of the internal field. In this way, the Rayleigh approximation method is acceptable and can be applied when the phase is also homogenous. However, for the phase to be the same both inside and outside the particle [8], (2) holds.

$$\frac{2\pi a}{\lambda}|\varepsilon - 1| \ll 1 \quad (2)$$

where

ε = the particle permittivity.

In defining what much less than 1 means in (2), 0.5 was set as the standard and limit. In this research work, the above assumptions and conditions were sampled for implementation. The values obtained from $k|\bar{m}|a$ and ka, for instance, at 100 GHz are, respectively, of the order of 0.4 and 0.2. Taking ε = 3.8 – j0.038 as the dielectric value, the third condition holds for wavelength of only millimetric range - order of frequency less than 85 GHz.

Furthermore, the Rayleigh scattering method is again verified against the Point-Matching Technique (PMT) which is a full solution of Maxwell's main equations. The PMT is a numerical method reputed for its very high accuracy. It is found that the agreement between the PMT method and the Rayleigh approximations method is good and acceptable as will be shown in section 4. Therefore, difficult calculations are avoided by using approximations such as the Rayleigh method while the fidelity of the process is not compromised.

The outputs of the absorption and the scattering cross sections can be obtained from the following equations:

$$\sigma_{abs} = \frac{8\pi^2 a^3}{\lambda} I_m\left(\frac{\varepsilon-1}{\varepsilon+2}\right) \quad (3)$$

$$\sigma_{sca} = \frac{8}{3}\pi^5\left(\frac{2}{\lambda}\right)^4 a^6\left|\frac{\varepsilon-1}{\varepsilon+2}\right|^2 \quad (4)$$

where

σ_{abs} = the absorption cross section
σ_{sca} = the scattering cross section
I_m = the imaginary part of relative complex permittivity

It follows, from (1), that for most particles in the Rayleigh approximation method, the expression in (5) yields:

$$\sigma_{abs} \gg \sigma_{sca} \quad (5)$$

given that $I_m\varepsilon$ is not very small for a frequency.

Furthermore, in this approximation, the total cross-section or extinction is given by:

$$\sigma_{ext} = \sigma_{sca} + \sigma_{abs} \quad (6)$$

For PMT, expressions in (7) and (8) are precisely satisfied in the boundaries exterior to the dust particle.

$$\nabla \times E + j\omega\mu H = 0 \quad (7)$$

$$\nabla \times H - (\sigma + j\omega\varepsilon)E = 0 \quad (8)$$

This is a treatment like the one carried out by [10]. The forward scattered amplitudes $(\theta = 0)$ for vertical and horizontal polarizations are expressed in (9) and (10):

$$S_v(0) = \frac{1}{E_v}\sum_{m=-\infty}^{\infty}\sum_{n\geq|m|}^{\infty}(-j)^{n-1}\, x\left[a_{mn}^{v}\frac{m}{\sin\tau}P_n^{|m|}(\cos\tau) + b_{mn}^{v}\frac{dP_n^{|m|}(\cos\tau)}{d\tau}\right] \quad (9)$$

$$S_h(0) = \frac{1}{E_h}\sum_{m=-\infty}^{\infty}\sum_{n\geq|m|}^{\infty}(-j)^{n+2}\, x\left[a_{mn}^{h}\frac{dP_n^{|m|}(\cos\tau)}{d\tau} + b_{mn}^{h}\frac{m}{\sin\tau}P_n^{|m|}(\cos\tau)\right] \quad (10)$$

where

τ = the incidence angle between the direction of wave propagation and the axis of symmetry.
$P_n^{|m|}$ = Legendre functions of the first kind.

3. ATTENUATION AND PHASE ROTATION MODELS

For polarized incident fields (vertical and horizontal), the attenuation ($A_{V,H}$) and phase rotation ($\beta_{V,H}$) can be respectively expressed as:

$$A_{V,H} = I_m\left[K_{V,H}(\alpha)\right] \quad (11a)$$

$$= kI_m(\bar{m})\,[Np/m]$$

where
k = the free space phase constant
$\bar{m}$ = the refractive index

Alternatively, the attenuation can be expressed as

$$A_{V,H} = kI_m(\bar{m})8.686 \times 10^3\,[dB/km] \quad (11b)$$

For the phase rotation, it is similarly expressed as shown in (12):

$$\beta_{V,H} = R_e\left[K_{V,H}(\alpha)\right] \quad (12a)$$

$$= kR_e(\bar{m})[rad/m]$$

or

$$\beta_{V,H} = kR_e(\bar{m})\left(\frac{180}{\pi}\right)\cdot 10^3[deg/km] \quad (12b)$$

Thus, in deriving the microwave attenuation and phase rotation in SDS, the definition of complex refractive index of a scattering medium denoted with $\bar{m}$ is given [11]:

$$\bar{m} = 1 - j2\pi k^{-3}NS(0) \quad (13)$$

where
N = the number of particles per cubic meter
$S(0)$ = the complex forward scattering amplitude function.

The propagation path may be said to be intersected by a slab having many dust particles. The field will be affected by scattering from the particles at a point, but the forward propagating wave is consistently affected only in the active region of the slab. The complex forward direction scattering is expressed as follows:

$$S(0) = jk^3p_s \quad (14)$$

where

p_s = the particle dipole's complex polarizability.

It is to be mentioned that the propagation constants depend on the scattering particles' shape as well as their orientation with respect to the polarization of the wave. The complex polarizability can be related to the complex permittivity and the particle's volume, v, using Mosotti-Lorentz-Lorenz equation, if the shape of the particles is considered as spheres.

$$p_s = \frac{3v}{4\pi}\left(\frac{\varepsilon-1}{\varepsilon+2}\right) \quad (15)$$

where

$$v = \frac{4}{3}\pi a^3 \quad (16)$$

where
ε = the dielectric constant
a = the radius of the spherical scatterer.

Let

$$G = \left(\frac{\varepsilon-1}{\varepsilon+2}\right) = G' - \mathrm{j}G'' \quad (17)$$

Eq. (16) and (17) can be substituted into (15) such that (14) becomes

$$S_s(0) = jk^3Ga^3 \quad (18)$$

Upon substituting (17) and (18) into (13) and by introducing the output to (11) and (12) respectively, the following equations are derived:

$$A = k.I_m[1 + 2\pi.a^3.N.G]\,[Np/m] \quad (19)$$

The attenuation equation expressed in (19) can be rearranged and further expressed in the following way:

$$A = 2\pi.k.a^3.N[I_m(G)]\,Np/m$$
$$= 39.478.\frac{a^3}{\lambda}.N\left[[I_m(G)]\right](8.686)\,[dB/m]$$
$$= 3.429 \times 10^5.\frac{Na^3}{\lambda}[I_m(G)]\,[dB/km] \quad (20)$$

The phase rotation component is also similarly treated to give the following expressions:

$$\beta = 2\pi.k.a^3.N[R_e(G)]\,[rad/m]$$
$$= 39.478.\frac{a^3}{\lambda}.N[R_e(G)]\left(\frac{180}{\pi}\right)\,[deg/m]$$
$$= 2.262 \times 10^6.\frac{Na^3}{\lambda}[Re(G)]\,[deg/km] \quad (21)$$

where
λ = the wavelength (m)
a = the radius (m)
N = dust concentration or the number of particles per unit volume
$Re(G)$ = the complex permittivity's real part
$I_m(G)$ = the complex permittivity's imaginary part defined in (17).

It is seen that the attenuation and the phase rotation coefficients as derived in (20) and (21) are in terms of particle radius, wavelength and number of particles. But the number of particles (per unit volume) is

a parameter difficult to measure in SDS. Effort is thus made to relate the concentration numbers of particles with visibility since SDS are usually meteorologically characterized and observed using visibility. Therefore, evaluating attenuation and phase rotation in SDS is treated further in this work in terms of visibility.

An expression relating dust concentration and visibility was given by [12], [13] and [14]. The expressions provide opportunity of application to different SDS characteristics. This also include a way of evaluating dust particle concentrations from the SDS visibility. These different expressions have been used by researchers, however another expression reported in Part II is:

$$N = \frac{2.250\times10^{-9}}{a^3 V^{\gamma}} \quad (22)$$

where

a = the equivalent particle radius in meters.

An equivalent particle radius was found to be 7.2 - 15.3 µm in particle size distribution functions from the work carried out by [9]. Therefore, an average value of 11.25 µm is adopted in this work where necessary.

3.1 Attenuation and phase rotation in spherical particles medium

In this section, attenuation and phase rotation models are treated by assuming that dust particle shape is spherical. The formulation of the model is treated for cases of monodisperse or equi-sized particle medium and polydisperse or particle size distribution medium.

a) Monodisperse medium

In a medium considered to be monodisperse in nature, the attenuation and the phase rotation coefficients are derived by recalling (20) and (21) and then substituting for N:

$$A = \frac{7.715\times10^{-4}}{\lambda V^{\gamma}} \cdot I_m(G)[dB/km] \quad (23a)$$

or

$$A = 2.572 \times 10^{-3} \cdot \frac{f}{V^{\gamma}} \cdot I_m(G)[dB/km] \quad (23b)$$

For the phase rotation component,

$$\beta = \frac{5.090\times10^{-3}}{\lambda V^{\gamma}} R_e(G)[deg/km] \quad (24a)$$

or

$$\beta = 1.697 \times 10^{-2} \cdot \frac{f}{V^{\gamma}} . R_e(G)[deg/km] \quad (24b)$$

where
f = the frequency in GHz.

In this way, attenuation and phase rotation in monodisperse medium are given, each, as a function of visibility - a realistic parameter often used in meteorology.

b) Polydisperse medium

Another realistic condition that a distribution of dust particle sizes exists necessitated the treatment of the attenuation and the phase rotation under polydisperse medium. Investigation [15] has shown that some particle radii are in exponential distribution form.

$$p(a) = \beta\, exp(-\beta a) \quad (25)$$

With a mean value $a = 1/\beta$ and $n(a) = N\, p(a)$,

$$n(a) = N\beta e^{-\beta a} \quad (26)$$

Given a particle size distribution (PSD), the propagation coefficient, K, can be shown to be:

$$K = k\left[1 + \frac{12\pi N}{\beta^3} G\right] \quad (27)$$

Substituting (27) into (11) and then substituting the product into (12),

$$A = 2.057 \times 10^6 \cdot \frac{N}{\lambda\beta^3} \cdot I_m(G) \quad [dB/km] \quad (28)$$

The phase rotation component can be similarly expressed as:

$$\beta = 1.357 \times 10^7 \cdot \frac{N}{\lambda\beta^3} \cdot R_e(G)[deg/km] \quad (29)$$

Lastly, the mean value a and (22) are used in deriving the attenuation and the phase rotation in polydisperse medium in terms of frequency and visibility.

$$A = 1.543 \times 10^{-2} \cdot \frac{f}{V^{\gamma}} \cdot I_m(G)\ [dB/km] \quad (30)$$

and

$$\beta = 1.018 \times 10^{-1} \cdot \frac{f}{V^{\gamma}} \cdot R_e(G)[deg/km] \quad (31)$$

4. RESULTS AND DISCUSSIONS

This section presents and discusses the results. The Rayleigh approximation technique is examined and validated for its accuracy and veracity. After their derivations, the proposed microwave models are also compared with similar existing models [9, 14 and 16]. Also, the models are implemented, and the results obtained are discussed and analyzed.

4.1Rayleigh technique validation

The Rayleigh approximation method is first validated using the PMT. By solving (9) and (10), the complex forward direction scattering given in (14) is validated against the Maxwell's full solution. The numerical accuracy and convenient way of determining

the unknown coefficients necessitated the choice of the PMT method.

In Table-1, the results for the horizontal as well as the vertical polarizations are presented.

It is important to note the very good concurrence between the two methods for both horizontal and vertical polarizations. The relative error for the two polarizations is less than 1% and 0.4% in the real and the imaginary parts, respectively.

Table-1. Rayleigh technique validation against PMT.

Method	Scattering amplitude – vertical, $S_v(0,\alpha)$	Scattering amplitude – horizontal, $S_h(0,\alpha)$	Minor axis radius (mm) (c)	Eccentricity c/a
Rayleigh scatterer	$9.541 \times 10^{-12} - j3.287 \times 10^{-10}$	$1.287 \times 10^{-11} - j3.812 \times 10^{-10}$	0.0031	0.8
	$7.289 \times 10^{-11} - j2.510 \times 10^{-9}$	$9.835 \times 10^{-11} - j2.912 \times 10^{-9}$	0.0063	0.8
	$5.569 \times 10^{-10} - j1.918 \times 10^{-8}$	$7.514 \times 10^{-10} - j2.225 \times 10^{-8}$	0.0125	0.8
	$4.225 \times 10^{-9} - j1.465 \times 10^{-7}$	$5.741 \times 10^{-9} - j1.700 \times 10^{-7}$	0.025	0.8
	$3.251 \times 10^{-8} - j1.119 \times 10^{-6}$	$4.386 \times 10^{-8} - j1.299 \times 10^{-6}$	0.050	0.8
	$2.485 \times 10^{-7} - j8.545 \times 10^{-6}$	$3.352 \times 10^{-7} - j9.928 \times 10^{-6}$	0.100	0.8
	$1.900 \times 10^{-6} - j6.529 \times 10^{-5}$	$2.579 \times 10^{-6} - j7.600 \times 10^{-5}$	0.200	0.8

Method	Scattering amplitude – vertical, $S_v(0,\alpha)$	Scattering amplitude – horizontal, $S_h(0,\alpha)$	Minor axis radius (mm) (c)	Eccentricity c/a
PMT	$9.465 \times 10^{-12} - j3.274 \times 10^{-10}$	$1.277 \times 10^{-11} - j3.798 \times 10^{-10}$	0.0031	0.8
	$7.252 \times 10^{-11} - j2.500 \times 10^{-9}$	$9.756 \times 10^{-11} - j2.900 \times 10^{-9}$	0.0063	0.8
	$5.524 \times 10^{-10} - j1.911 \times 10^{-8}$	$7.454 \times 10^{-10} - j2.216 \times 10^{-8}$	0.0125	0.8
	$4.221 \times 10^{-9} - j1.453 \times 10^{-7}$	$5.695 \times 10^{-9} - j1.169 \times 10^{-7}$	0.025	0.8
	$4.358 \times 10^{-8} - j1.300 \times 10^{-6}$	$4.358 \times 10^{-8} - j1.300 \times 10^{-6}$	0.050	0.8
	$3.364 \times 10^{-7} - j9.940 \times 10^{-6}$	$3.364 \times 10^{-7} - j9.940 \times 10^{-6}$	0.100	0.8
	$2.579 \times 10^{-6} - j7.600 \times 10^{-5}$	$2.579 \times 10^{-6} - j7.600 \times 10^{-5}$	0.200	0.8

4.2 Proposed models validation

In this section, the newly proposed models (expressed in (23) & (24) and (30) & (31) are validated against existing models, having confirmed the veracity of the adopted method in formulating the models. Both the proposed models and the existing models are also simulated, and the results obtained are presented in this section.

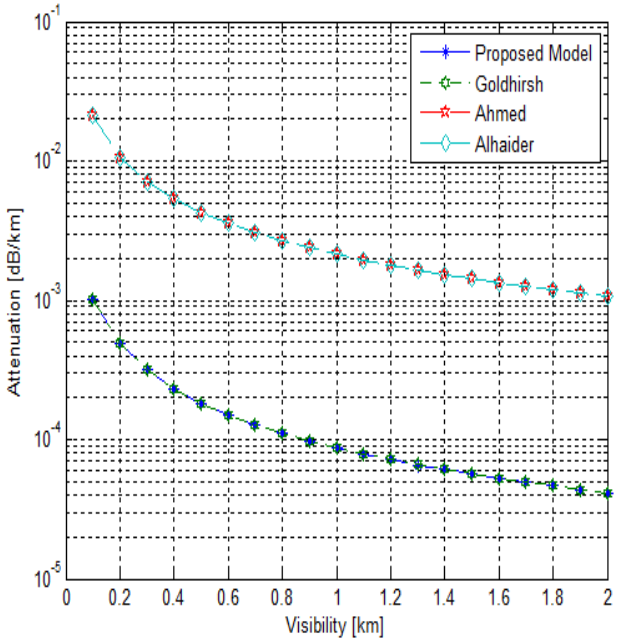

Figure-1. Validation of proposed model.

To validate the proposed microwave attenuation and phase rotation models, permittivity, $\varepsilon = 3.8 - j0.038$ and wavelength, $\lambda = 0.03m$ are used except where it is, perhaps, stated otherwise. Figure-1 clearly illustrates the proposed model validation i.e. (23). The relative ease of setting attenuation against visibility was a factor that necessitated the selection of Ahmed, Alhaider and Goldhirsh's models.

Very good agreement in the results obtained by the new model and the existing models especially that of [14] is recorded. However, a somewhat lesser agreement is seen in the case of [9] and [16] models. This may be due to the optical attenuation coefficient and the constant ratio used by these authors in relating visibility with dust concentration. Of all the microwave attenuation models investigated, [9] and [16] models present higher attenuation value, while the Goldhirsh and the new formulated models have lower microwave attenuation values.

From conceptualization stage to formulation stage, the proposed models explore the drawbacks of existing models and important consideration hitherto not included in the existing microwave attenuation models. This includes the different transmission media (monodisperse and polydisperse) as well as the relation of particle concentration and visibility. The models being proposed are easy to apply making it possible to avoid rigorous method of computations that are common in numerical methods such as the PMT. The readily available parameters in which the proposed models are given is also another advantage. Lastly, another pointer to the higher accuracy of the models being proposed in this work is the different veracity stage which the method was made to go through.

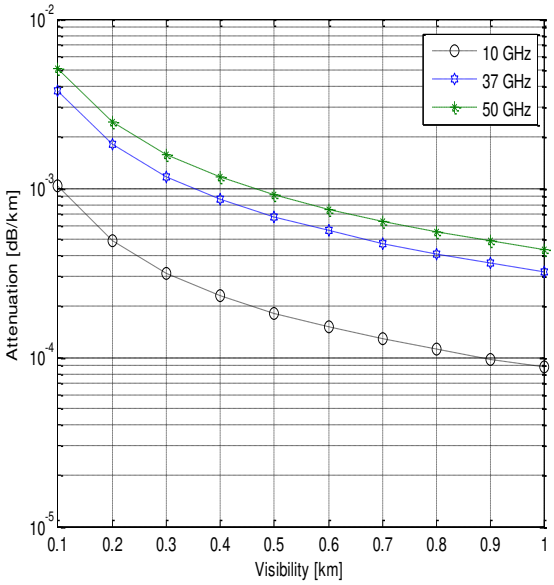

Figure-2a. Attenuation versus visibility at different frequency.

4.3 Models implementation

The microwave attenuation and phase rotation are, in this section, implemented having validated the proposed models. As shown in Figure-2a and Figure-2b, attenuation and phase rotation have been plotted for different visibility range (100m to 1,000m) using (23) and (24), respectively. The results show a linear dependence on visibility and frequency. It is observed that the attenuation is heightened as the SDS get worsened. However, increase in visibility during SDS decreases the attenuation.

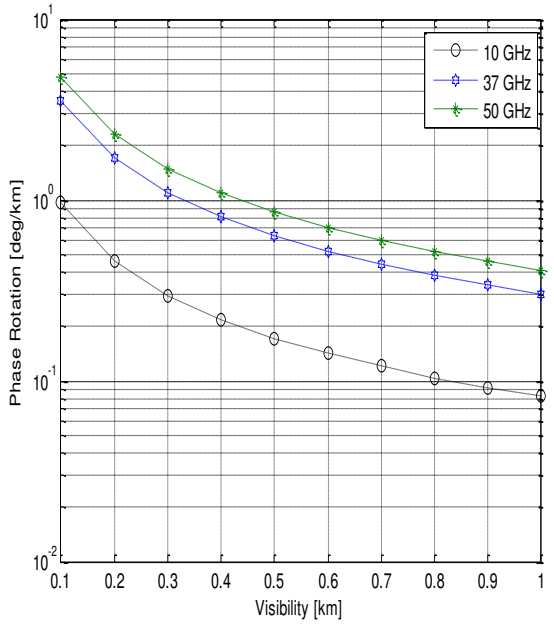

Figure-2b. Phase rotation versus visibility at different frequency.

Suffice to mention that attenuation could be very high when visibility is around 1m. When the visibility is at 100m, the attenuation varies between 0.001dB/km, 0.0038dB/km and 0.005dB/km as the frequency varies between 10GHz, 37GHz and 50GHz, respectively. An important definite conclusion to be drawn is that SDS affect microwave signal at higher frequency since phase rotation and attenuation increase with increase in frequency.

Furthermore, microwave attenuation is also checked when complex permittivity varies at different moisture content, and at frequency of 10GHz. The results obtained when moisture content is 0% and permittivity is 2.53 - j0.0625 as well as when moisture content is 10% and permittivity is 4.0 - j01.325 are shown. At visibility of 0.1km, the attenuation is 0.010dB/km for 0% (i.e. dry) and is 0.116dB/km for 10% moisture. This means that attenuation increases markedly with increase in moisture as shown in Figure-3.

The reason for the increase in attenuation can be attributed to the fact that dust particles that are moist usually induce changes of the particles dielectric constant. Therefore, dust storms with high moisture will experience greater signal fading and attenuation effects than those with lower moisture content. This means that higher attenuation values are possible in tropical areas with high humidity when compared with semi-arid and desert regions.

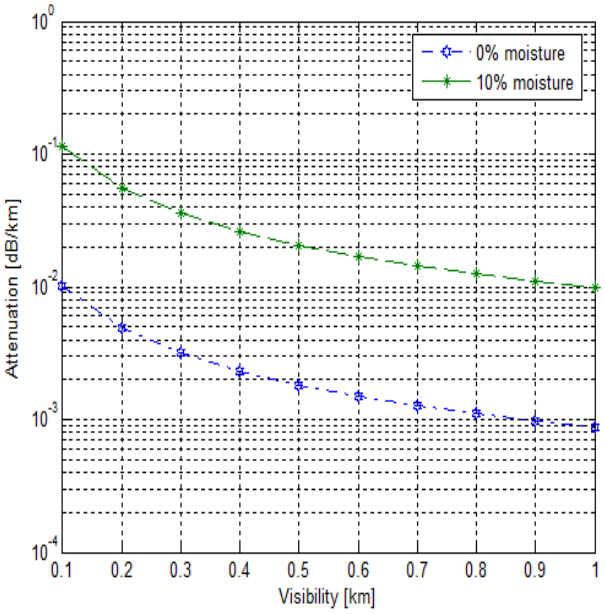

Figure-3. Attenuation versus visibility at different moisture content.

As shown in Figure-4 and Figure-5, the results obtained after implementing the proposed model when particle size distribution is considered are also presented. It is found, going by the proposed model in (30) that the attenuation caused by dust particles of exponential distribution is higher than the attenuation caused by dust particles for mono-sized distribution. This also becomes

apparent when Figure-2a (monodisperse medium) is compared with Figure-4 (polydisperse medium).

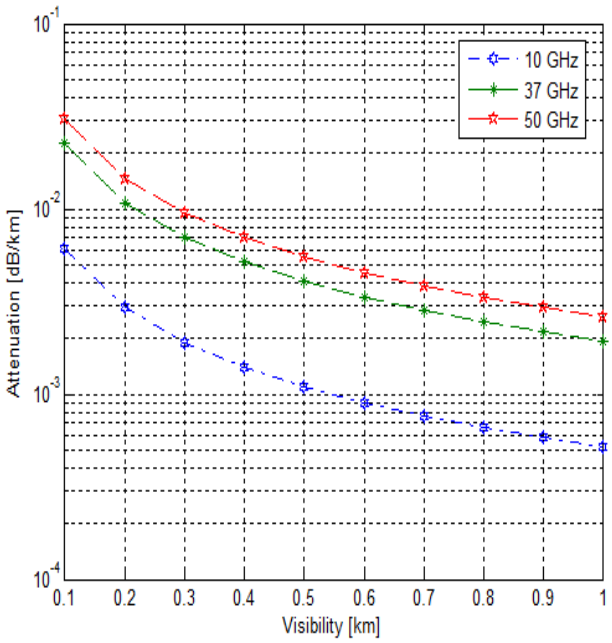

Figure-4. Attenuation versus visibility (polydisperse medium).

At different frequency range, Figure-5 shows a comparison between microwave attenuation for equi-sized particles and dust particle sizes distribution using (23) and (30) respectively.

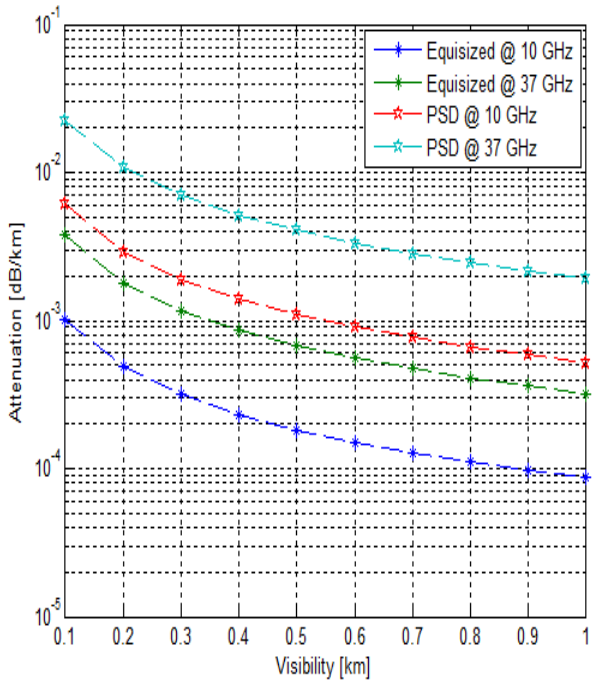

Figure-5. Attenuation versus visibility with equi-sized particles and PSD.

5. CONCLUSIONS

In this research work, models to predict phase rotation and microwave attenuation due to dust particles have been developed under different conditions. The adopted method was verified for reliability and accuracy of the developed models. Also, comparison was made between the new models and the existing ones. Good performance and excellent conformity was observed.

Unlike the existing models, the models being proposed were derived by paying attention to particle concentration and its relationship with SDS visibility. The proposed models also considered particle shape in both monodisperse and polydisperse media. The models were developed in terms of visibility, frequency and dielectric constant in a way that rigorous computations could be avoided; making it an added advantage of the models.

The microwave attenuation and phase rotation caused by moistened and dry dust particles have been determined for different frequency and visibility. There is an increase in attenuation as moisture content increases. Similarly, attenuation and phase rotation are directly proportional to frequency but are inversely proportional to the SDS visibility. There is an increase in attenuation as the frequency increases and the visibility decreases. The microwave attenuation becomes significant during serious SDS but may be said to be negligible as the visibility in SDS improves.

REFERENCES

[1] Q. Dong, L. Wang, L. Yingle, M. Wang, X. Jiadong and B. Wang. 2013. Effect of charged sand particles on microwave propagation along earth-space paths. International Conference on Remote Sensing, Environment and Transportation Engineering. 681-684.

[2] M. M. Chiou and J.-F. Kiang. 2016. Attenuation of millimeter-wave in a sand and dust storm. IEEE Geosci. Remote Sens. Lett. 13(8): 1094-1098.

[3] A. Musa, S. O. Bashir and A. H. Abdalla. 2014. Review and assessment of electromagnetic wave propagation in sand and dust storms at microwave and millimeter wave bands-Part I. Prog. Electromag. Res. M. 40: 91-100.

[4] M. F. Kahnert. 2003. Numerical methods in electromagnetic scattering theory. Journal of Quantitative Spectroscopy & Radiative Transfer. 79(80): 775- 824.

[5] Q. Dong, L. Ying-Le, X. Jia-dong, H. Zhang and M. Wang. 2013. Effect of Sand and Dust Storms on Microwave Propagation. IEEE Transactions on Antennas and Propagation. 61(2).

[6] Y. Wenyan and X. Jingming. 1990. Cross polarization effect of circularly polarized microwave, millimeter wave propagation in the air suspending dust particles. Chinese J. Radio Sci. 5: 44-50.

[7] Q. Dong, J.D. Xu, Y.L. Li, H. Zhang and M. Wang. 2011. Calculation of Microwave Attenuation Effect Due to Charged Sand Particles. J. Infrared Milli Terahz Waves. 32, 55-63.

[8] S. O. Bashir. 2008. Electromagnetic scattering computation methods for very small particles: Part II. Intern. Conf. on modelling & simulation, Published in MS Journal. 9(1-2-3).

[9] A. S. Ahmed. 1987. Role of particle-size distributions on millimeter-wave propagation in sand/duststorms. Inst. Electr. Eng. Proceedings. 134, 55-59.

[10] J. A. Morrison and M. J. Cross. 1974. Scattering of Electromagnetic Waves by Axisymmetric Rain Drops. The Bell System Technical Journal, USA. 53(6): 955-1019. 6.

[11] H. C. Van de Hulst. 1981. Light Scattering by Small Particles. New York, John Wiley and Sons. (Reprinted 1981, Dover Publications, Inc., New York).

[12] W. S. Chepil and N. P. Woodruff. 1974. Sedimentary Characterisation of Duststorms: II-Visibility and Dust Concentration. American Journal Sci. Vol. 255.

[13] D. A. Gillett. 1979. Environmental factors affecting dust emission by wind erosion. C. Morales, Ed. New York: Wiley.

[14] J. Goldhirsh. 2001. Attenuation and backscatter from a derived two-dimensional duststorm model. IEEE Transactions Antennas Propagation. 49(12): 1703-1711.

[15] S. Ghobrial. 1980. Effect of sand storms on microwave propagation. National Telecommunication Conference, Houston, Texas. pp. 43.5.1- 43.5.3.

[16] M. A. Alhaider. 1986. Radio wave propagation into sandstorms system de- sign based on ten-years visibility data in Riyadh, Saudi Arabia. Int. J. Inf. Millim. Waves. 7: 1339-1359.